# Ultrathin films in wetting evidenced by x-ray reflectivity

J. Daillant and J. J. Benattar
*Service de Physique du Solide et de Résonance Magnétique, Direction de la Physique, Centre d'Etudes Nucléaires de Saclay, 91191 Gif-sur-Yvette CEDEX, France*

L. Leger
*Physique de la Matière Condensée, Collège de France, 11 Place Marcelin-Berthelot, 75231 Paris CEDEX 05, France*
(Received 6 July 1989)

The role of thin films in different situations of wetting has been investigated by x-ray reflectivity, a technique that allows an independent determination of their thicknesses, densities, and roughnesses, using a nonvolatile siloxane oil spreading on different kinds of surfaces. The spreading of a microscopic droplet involves at least two stages: the development of a "tongue" of molecular thickness controlled by the spreading parameter and the friction on the substrate is followed by a surface diffusion process. The final stages of spreading are shown to be largely dependent on the polymer-substrate interactions. Increasing the chain length of the polymer slows the process down, but does not lead to a qualitatively different behavior. This study has been complemented with capillary rise experiments in order to measure diffusion constants. The results are discussed using a simple model of surface flow.

## I. INTRODUCTION

Beyond the classical theory of capillarity, the role of thin films must be carefully considered in order to understand the fundamental processes involved in the phenomena of wetting.[1,2] This role is by no means restricted to the final stages; Hardy[3] discovered the existence of a precursor film extending ahead of a spreading droplet and attributed it to a transfer process via the vapor. A precursor film has since been detected with liquids that are clearly nonvolatile[4] and the present study will be restricted to this case.

Thin films are either of molecular or "colloidal" thickness. In this latter case, the thickness (controlled by electrostatic forces, dispersive forces, etc.), ranges from a few nanometers to hundreds of nanometers. This situation has been extensively studied by de Gennes[5] and Joanny[6] for two classical cases: the spreading of a droplet and the capillary rise. Here, the relevant parameters are the surface tension of the liquid $\gamma$, the spreading parameter $S$ (which measures the energy gained by unit surface when the liquid covers the solid substrate) and, in the case of van der Waals liquids, the effective Hamaker constant $A$ (which measures the strength of dispersive forces). If $S \geq 0$, spreading spontaneously occurs (i.e., complete wetting). High-energy surfaces have a large-$S$ value whereas low-energy surfaces have a low-$S$ value. Following the theoretical results, when $\langle S/\gamma \rangle^{1/2} \ll 1$ only films of colloidal thickness are present, and an entirely hydrodynamic theory can be developed; all films are truncated at a thickness $[A/(4\pi S)]^{1/2}$, which is larger than the molecular dimensions. Conversely, we shall show that, if $\langle S/\gamma \rangle^{1/2} \lesssim 1$, a part of the films will be of molecular thickness and one must take into account surface diffusion. This corresponds to the practical situations.

In early studies, thin films were characterized indirectly by effects related to their presence: friction,[3] electrical conductivity,[7] size effects,[8] etc. More recently, ellipsometric measurements[9-12] have permitted a quantitative study of precursor films.

X-ray reflectivity measurements allowed the first determination of the final stages of spreading.[13] This technique, known to be a powerful tool in the field of surface physics, was shown to be a most sensitive means to investigate very thin wetting films involving complex density profiles (the role of surface roughness must be taken into account). The surface roughnesses of solids[14] or simple liquids[15,16] and the determination of the structure of organic layers (on water,[17,18] transferred[19,20] or grafted[21,22]) or of inorganic superlattices[23,24] are examples of problems which have been tackled using x-ray reflectivity. It can be applied to more complicated situations in physical chemistry where these two aspects are implicated. Moreover, we have shown that, using a sufficiently collimated beam, it is possible to study samples whose properties vary from place to place over the surface, allowing one to investigate new experimental situations with this technique. Let us remark that, in the range of thicknesses from 0.1 to 100 nm, x-ray reflectivity is unique within optical sciences in allowing an independent and simultaneous determination of thicknesses (given by the location of interference minima), of densities, and of roughnesses (related to the absolute intensities). An important point to be emphasized is that a precise determination of all these three quantities is required in order to get a relevant description of the phenomena at a molecular level.

The aim of this present work is to study the dynamics and to determine the mechanisms of spreading of microscopic droplets from their deposition until the final stages. For this purpose, it would be of great advantage to be able to compare the situations occurring with different molecular weights of a polymer and, above all, with different kinds of substrates. These comparisons are

 

allowed by the precise data obtained from x-ray experiments. Consequently, we have studied very small, clearly nonvolatile, siloxane drops, deposited on silicon wafers either after cleaning or after coverage by a self-assembling silane layer.[25] We also report on capillary rise experiments undertaken with the same polymer. The two substrates are well representative of high- and low-energy surfaces, and they are expected to be indicative of a wide range of situations. The macroscopic scaling laws have been verified on this system[4] by ellipsocontrast microscopy; the precursor film has been characterized by ellipsometry[10] and appears, except for the kinetics, in agreement with theoretical predictions.[26,27] Our previously published x-ray reflectivity results[13] allowed the determination of the final stages of spreading on this same model system.

A presentation of the x-ray grazing incidence techniques will first serve to make clear what kind of information can be extracted from the experimental data and how these techniques are suited to the study of thin wetting films. The results of the x-ray experiments on the spreading of microscopic polymer droplets of different molecular weights on low- and high-energy substrates, complemented with capillary rise experiments, will then be detailed. It appears that the leading mechanism occurs at a molecular level, and we shall try to discuss the results, taking into account the polymer-substrate interactions, with a simple model of surface flow.

## II. X-RAY OPTICS

All the experiments reported in the present paper have been performed with a four-circle diffractometer which was specially designed to carry out surface diffraction experiments together with x-ray reflectivity experiments. (This instrument will be detailed in Sec. III.) When used together, these two techniques allow a complete determination of the structure of a surface film. To follow the spreading of a droplet, x-ray reflectivity, which provides information normal to the substrate plane, will be the most useful; surface diffraction is used to precisely determine the structural properties of one kind of substrate.

### A. X-ray reflectivity

The geometry is shown schematically in Fig. 1(a); the corresponding wave-vector transfer $\mathbf{q}$ is perpendicular to the surface of the substrate ($\mathbf{q}=q_z\hat{\mathbf{z}}$), thus giving information on the projection of the electron density $\rho(z)$ onto the normal to this surface ($\hat{\mathbf{z}}$).

For x-ray wavelengths, the refractive index $n$ is such that $n=1-\delta+i\beta$; $\delta\approx 10^{-6}$ is proportional to the electron density $\rho$ and $\beta$ to the linear absorption coefficient.[28] Since the real part of the index is less than 1, total external reflection occurs for angles of incidence below a critical angle $\theta_c=\sqrt{2\delta}$. Beyond the critical angle, for a single ideal diopter the reflected intensity follows the Fresnel law.

#### *1. First Born approximation*

If the angle of incidence $\theta$ is sufficiently greater than $\theta_c$, multiple scattering may be neglected; the equivalent

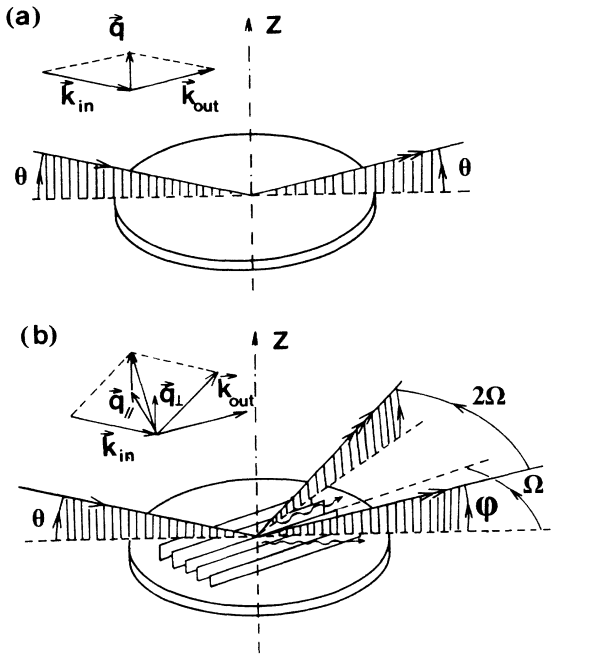


FIG. 1. (a) Geometry for reflectivity studies. (b) Geometry for surface diffraction experiments. The evanescent wave is diffracted by planes normal to the surface.

of the first Born approximation in quantum theory becomes very accurate[29] and provides a transparent means to understand the reflectivity curves. In this approximation, the reflectivity averaged on the coherence of the beam is given by[30,16]

$$\langle R(q_z)\rangle = R_F(q_z)\left\langle \left| \frac{1}{\rho_s}\int dz\, e^{iq_z z}\frac{\partial\rho(z)}{\partial z}\right|^2\right\rangle , \qquad (1)$$

where $q_z$ is the projection of $\mathbf{q}$ onto $\hat{\mathbf{z}}$ and $\rho_s$ the electron density of the substrate; $R_F(q_z)$ is the Fresnel reflectivity of the substrate surface, i.e., the reflectivity, as given by the Fresnel formulas,[31] of a perfect diopter having the bulk density of the substrate. Equation (1) is subject to two kinds of limitations: Firstly, the Born approximation requires small scattering cross sections (and this is verified for $\theta\gtrsim 3\theta_c$); secondly, the density gradients must be small as compared to the wavelength $[(1/k\rho)(\partial\rho/\partial z)\approx(2\pi)^{-3/2}\lambda/\langle z^2\rangle^{1/2}\approx 0.03$ for a roughness $\langle z^2\rangle^{1/2}=0.3$ nm].[16] Obviously, the shape of the reflectivity curves [Eq. (1)] results from interferences between the beams reflected by large electron density gradients (i.e., the surface and different interfaces).

We shall present below results of polymer droplets deposited on a substrate consisting of a silicon wafer covered by its natural oxide layer on which is eventually grafted a silane layer. As in many similar cases, the system can be described as composed of chemically homogeneous layers, and a model can be constructed by considering these layers as slabs of constant density. Then, one can take into account the roughness of an interface by smearing it through a convolution with a Gaussian function, assuming a random distribution for its position along $\hat{\mathbf{z}}$,[20] and this is a good approximation for $\theta\gtrsim 3\theta_c$:[14]

$$\langle R(q_z)\rangle = R_F(q_z)\left\langle \left| \frac{1}{\rho_s}\int dz \sum_{i=1}^{n} \frac{1}{\sqrt{2\pi\langle z_i^2\rangle}}(\rho_i-\rho_{i-1})e^{iq_z z}\exp\left[-\frac{(z-z_i)^2}{2\langle z_i^2\rangle}\right]\right|^2\right\rangle , \quad (2)$$

where $z_i$ is the distance between the surface chosen as reference and the $i$th interface whose width is $\langle z_i^2\rangle^{1/2}$; $\rho_i$ is the electron density of the $i$th slab. Integrating by parts provides

$$\langle R(q_z)\rangle = R_F(q_z)\left\langle \left| \frac{1}{\rho_s}\sum_{i=1}^{n}(\rho_i-\rho_{i-1})e^{iq_z z_i} \times e^{-(1/2)q_z^2\langle z_i^2\rangle}\right|^2\right\rangle . \quad (3)$$

This reflectivity profile, calculated from the model, is then convoluted with the experimental resolution and fitted to the experimental data. The case of a single layer will make clear how information can be extracted from the data.

### 2. The case of a single layer

*a. Determination of thicknesses, densities, and roughnesses.* In the case of a single lamina, that of a polymer film on a homogeneous substrate, Eq. (3) becomes

$$\langle R_F(q_z)\rangle = R_F(q_z)\frac{1}{\rho_s^2}\left[\rho_l^2 e^{-q_z^2\langle z_l^2\rangle}+(\rho_s-\rho_l)^2 e^{-q_z^2\langle z_s^2\rangle}+\cdots+2\rho_l(\rho_s-\rho_l)e^{-(1/2)q_z^2(\langle z_s^2\rangle+\langle z_l^2\rangle)}\cos(q_z z_l)\right] . \quad (4)$$

In many cases, the interfaces are smooth and the $\langle z_i^2\rangle^{1/2}$ are smaller than the different thicknesses. At angles near the first negative interference, the minimum of the function is only slightly shifted by the multiplication with the Gaussian term since $q_z^2\langle z^2\rangle \simeq \pi^2\langle z^2\rangle/z^2 \leq 1$. Let us carefully examine this situation in the simple case of a single layer using formula (4): The thickness will be unambiguously determined by the location of the first destructive interference and the electron density by the absolute value of the contrast, provided $\rho_s$ is known. Note that since the electron density of many organic materials is approximately half of that of silicon, the contrast is maximum. The roughnesses are obtained by fitting the entire curve with the model. More generally, a very important feature of the technique in this case is that, contrary to the ellipsometry, the determination of the thicknesses is independent of that of the roughnesses and densities. Such a refined picture of thin films is possible due to the fact that the index is directly related to the local electron density.[32]

*b. The case of very thin films.* Very thin films (thickness $\lesssim \langle z_i^2\rangle^{1/2}$) will be of great importance in this paper. In this case, thicknesses and roughnesses may have the same order of magnitude and the film may be very inhomogeneous. A relevant physical quantity is then a surface excess quantity[33] $\Gamma$ which can easily be calculated using the model. In the case of a single layer on a substrate, for example,

$$\Gamma = \rho_l l , \quad (5)$$

where $\rho_l$ is the density of the layer, whose thickness is $l$. $\Gamma$ is simply the number of electrons per unit surface due to the film. This quantity enlightens another aspect of the problem: the amount of matter present at the interface is determined, whereas thicknesses, densities, and roughnesses give information about the distribution of this matter. Thus, comparing the two kinds of information, one can get indirect indication about the conformation of the molecules at the surface.

### 3. X-ray reflectivity on microscopic droplets

When studying droplets, a new difficulty arises in comparison with more conventional x-ray reflectivity studies since the thickness of the film is different at each point on the surface (Fig. 2). We have shown[13] that, using a sufficiently collimated beam, it is possible to determine the profile of a droplet. The main effect of the variations in the thickness over the illuminated area of the sample is a decrease in the contrast of the interference pattern. If the slope of the droplet is such that the height variations are of the order of magnitude of the thickness, the fringes completely disappear. Conversely, if the height variations over the coherence area of the beam[34] remain small as compared to the thickness of the film, one can estimate the reflectivity by averaging the reflectivities over the illuminated area. The size of this area of coherence on the sample is $\lambda^2 R^2/4\delta_x\delta_y\theta$, where $\lambda$ is the wavelength, $\delta_x$ and $\delta_y$ the width and the height of the source, $R$ the source to sample distance, and $\theta$ the angle of incidence. In general, the thickness variations are negligible over this area of size, here typically on the order of a tenth of a $\mu m^2$. In the case of a single layer, the reflectivity is given by Eq. (4) whose only thickness dependent term is $\cos(q_z z_l)$. Let us first examine the case of microscopic droplets. In our experiments, the illuminated area, determined as the intersection of the beam with the droplet surface, had a length normal to the droplet radius on which it is centered, and a width parallel to it [Fig. 2(a)]. For this geometry $z_l = z_0 + z_y' y - \frac{1}{2}z_x'' x^2$ over the illuminated area to lowest order in $x$ and $y$. $z_y'$ is the slope of the droplet surface along $y$ (the slope along $x$ is 0) and $z_x''$ its curvature along $x$. The average over the illuminat-

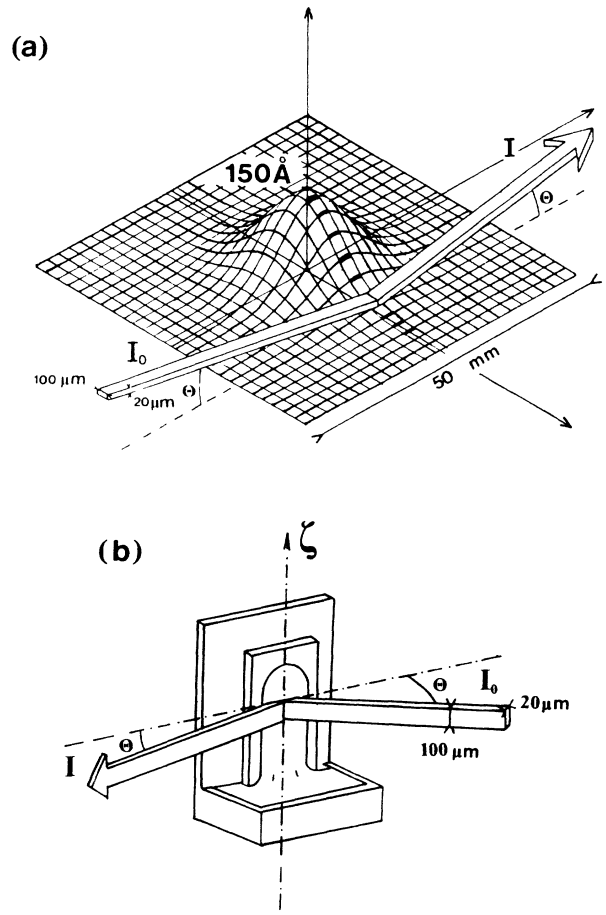


FIG. 2. Schematic view of (a) an x-ray experiment on a microscopic droplet and (b) a capillary rise experiment studied by x-ray reflectivity.

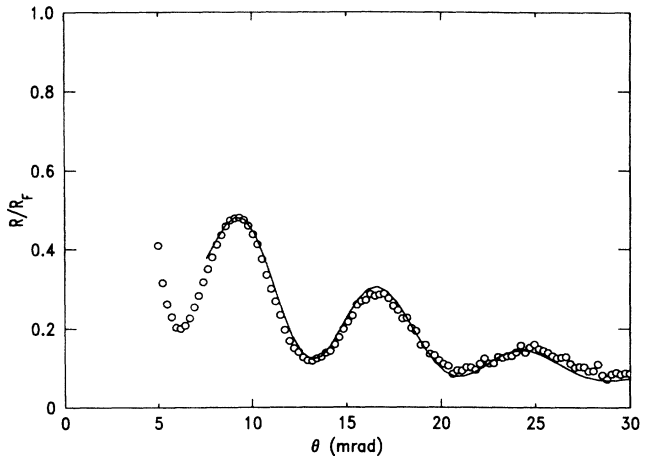


FIG. 3. Reflectivity curve recorded at the edge of a droplet. The mean thickness is 10 nm, the slope is 2 nm/mm, and the beam size is $20\times100$ $\mu m^2$. The contrast is much lower than for the case of a flat film [Fig. 5(a)].

ed area is therefore the real part of

$$\tfrac{1}{2}e^{iq_z z_0}\frac{\sin\theta}{\delta_x\delta_y}\int_{-\delta_y/2}^{\delta_y/2}dy\, e^{iq_z h'_y y}\int_{-\delta_x/2\sin\theta}^{\delta_x/2\sin\theta}dx\, e^{-(1/2)iq_z h''_x x^2},$$

in which the last term leads to Fresnel integrals and has to be numerically calculated. When the incident angle $\theta$ is increased, the length of the illuminated area is reduced and the observed mean thickness increases; consequently, the contrast increases and the interfringe distance slightly decreases. Such effects are apparent in the experimental data (Fig. 3) and must be taken into account when determining the film parameters. The agreement with the model is very satisfying using the parameters of the droplet as determined on the complete profile and the beam dimensions. In the case of the capillary rise [Fig. 2(b)] the contrast is not dependent on $\theta$, since the film is expected to be flat normal to its direction of growth.

### B. Surface diffraction

Surface diffraction has been first used by Marra, Eisenberger, and Cho[35] to study the surface of solids, and more recently it has been employed at the air-water interface.[36,37] Here we use this technique to characterize the complete structure of the substrates obtained by grafting a silane layer onto a silicon wafer. A highly collimated beam of x rays strikes the surface at an angle of incidence just under $\theta_c$; total external reflection occurs and an evanescent wave propagates parallel to the surface and is diffracted by planes normal to the surface [Fig. 1(b)]. This wave has a very small penetration (a function of the incident angle) and is thus highly selective for the first layers near the surface. The scattering pattern can be calculated from the distorted-wave Born approximation.[38] For a zero-thickness layer, the Bragg reflections should extend up to infinity in the third direction (Bragg rods); for a thin layer, the Bragg rods have a well definite profile[38,39] which condenses to a classical Bragg reflection as the thickness is increased. From the location and the width of the peak, one can determine the spacing of the diffracting planes (using the Bragg law) and a correlation length.[39]

## III. FOUR-CIRCLE DIFFRACTOMETER FOR SURFACE STUDIES

The experiments were carried out using a four-circle diffractometer (Fig. 4). This diffractometer allows us to carry out reflectivity, surface diffraction, and grazing incidence fluorescence measurements. This nonstandard apparatus was designed in our laboratory in collaboration with Microcontrôle, Evry, France. A conventional fine-focus copper-tube source is used. The Cu $K\alpha_1$ line is selected using a plane LiF(200) monochromator and the beam is collimated by a divergence slit $S_D$ (25 $\mu$m wide) providing a very low divergence ($\sim0.1$ mrad). A slit $S_H$ ($100\ \mu m < S_H < 5$ mm) can be used to limit the height of the illuminated area on the sample in order to probe only a small area, allowing the determination of the droplet profiles (Fig. 2). The scattered beam is detected by a scintillation counter placed behind the analysis slit $S_A$ (700 $\mu$m). The source-to-sample and the sample-to-detector

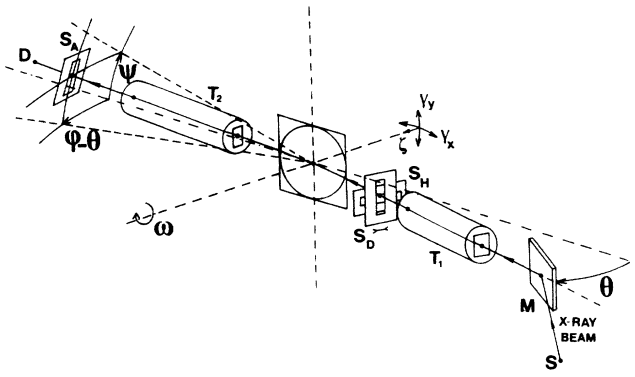


FIG. 4. The four-circle diffractometer for surface studies.

distances are both 40 cm.

The goniometric head $(\gamma_x,\gamma_y)$ and the translation $(\zeta)$ are used to position the sample surface at the center of the diffractometer, parallel to the beam sheet at $\theta=0$.

In this paper, we report surface-diffraction and -reflectivity experiments. In the case of surface diffraction, $\theta$ is fixed to an angle smaller than the critical angle of total external reflection $\theta_c$, and $\varphi$ and $\psi$ are moved to explore the Bragg rods. In the case of a two-dimensional powder $\omega$ may be kept fixed.

Reflectivity curves are recorded at $\psi=0$; $\varphi$ is scanned around $2\theta$ ($\theta$ is the incident angle) in order to measure the background which is then substracted. The intensity of the incident beam necessary to determine the absolute reflectivity was measured at low power, as well as the intensity for small incident angles. At greater incidences (including an overlap with the first zone) the x-ray tube is used at a higher power. The second part of the curve is fitted to the first allowing the determination of a ratio which is used to determine the primary intensity. Note that there is no change in diffractometer resolution.

It should be pointed out that, with this device, we could determine reflectivities lower than $10^{-8}$, providing direct information at a scale of approximately 0.4 nm. The limitation is due to the signal to background ratio and not to the brightness of the source. As a matter of fact, synchrotron radiation is not required to carry out such experiments. The counting time per point is not a limitation for experiments with such very slow dynamics. One may note, also, that our divergence of $10^{-4}$ corresponds to the $1/\gamma$ divergence of a synchrotron operated at 5 GeV.

## IV. EXPERIMENTAL DETAILS

### A. The siloxane oil

A nonvolatile liquid can be found with a polymer of sufficiently high molecular weight. The polydimethylsiloxane (PDMS) is liquid at room temperature. Pumping over a vessel containing the siloxane oil does not lead to any diminishing of the sample mass, and the volume of a droplet deposited on a surface that it does not wet, remains constant over months. The choice of a polymer is convenient, since the viscosity can be varied over a wide range through the choice of the molecular weight,[11] negligibly affecting the other characteristics of the liquid, especially the cohesive interactions. The samples were prepared by fractionated precipitation to eliminate small oligomers. The surface tension of this polymer is $\gamma\sim 20.5\pm 0.5$ mN/m at $T=20$ °C.[40] Its other characteristics, including the polydispersity index $M_W/M_N$, are listed in Table I.

As we shall see, the complete spreading of a PDMS droplet of molecular weight 6500 g/mol requires several months. This very long time (which becomes prohibitive with longer chains) is, in fact, the most serious limitation of such experiments but cannot be avoided if one wants liquids that are clearly nonvolatile. Consequently, attention has been focused on the spreading of PDMS of molecular weight 6500 g/mol on bare silicon.

It should be remarked that PDMS chains with a molecular weight greater than $\sim 13\,000$ g/mol are entangled so that a different behavior is possible for chains that are longer or shorter than this value, especially for the dynamics.

Horn and Israelashvili[41] have recently reported measurements of the force between two smooth mica surfaces immersed in liquid PDMS. Their results are indicative of a pinning of the polymer chains at the surfaces and, also, of a strong layering at small separations deduced from the observation of oscillations in the force between the surfaces having a period corresponding to the width of the dimethylsiloxane chain (about 0.7 nm).

### B. The substrates

Two kinds of substrates were used: clean and silanated silicon wafers corresponding to high and low spreading parameters. Each has been carefully characterized by x-ray techniques.

#### *1. Silicon wafers*

The first type of substrate was an optically polished (400) silicon wafer (50 mm in diameter and 2 mm thick, to ensure a good flatness) covered by its thin natural oxide layer (2 nm thick).

A high-energy surface is obtained by strong oxidation of the organic impurities through an oxygen flow under uv radiation.[42,43] This is an efficient cleaning procedure

TABLE I. Characteristics of the polymer samples: molecular weight $M_W$, polydispersity index $M_W/M_N$, viscosity $\eta$, and surface tension $\gamma$.

| $M_W$ (g/mol) | $M_W/M_N$ | $\eta$ (Pa s) | $\gamma$ (mN/m) |
|---|---|---|---|
| 6 500 | 1.8 | 0.05 | 20.5±0.5 |
| 9 600 | 1.45 | 0.09 | 20.5±0.5 |
| 33 000 | 1.15 | 1.15 | 20.5±0.5 |
| 50 000 | 1.15 | 4.5 | 20.5±0.5 |
| 79 000 | 1.15 | 20.5 | 20.5±0.5 |

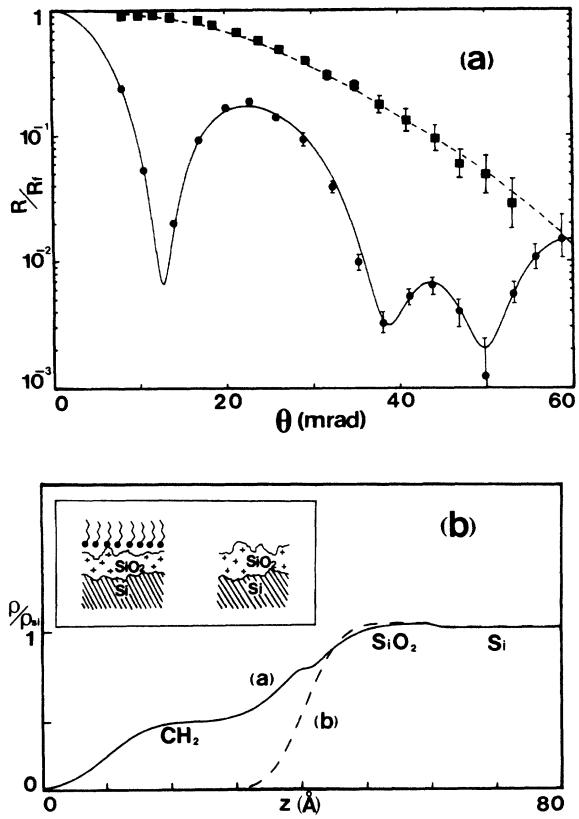


FIG. 5. (a) Reflectivity curves (divided by the Fresnel reflectivity of the substrate): closed square, bare silicon; closed circle, silanated silicon recovered by a PDMS monolayer. The dotted and solid lines indicate the least-squares fits. (b) Electron density profiles corresponding to the fit of the reflectivity curves represented in (a). Dotted line: bare silicon ($\langle z^2\rangle^{1/2}=0.42\pm0.05$ nm), solid line: silanated wafer ($\langle z^2\rangle^{1/2}=0.36\pm0.03$ nm for the silane-air interface, $\langle z^2\rangle^{1/2}=0.47\pm0.05$ nm for the silane–dense-layer interface and $\langle z^2\rangle^{1/2}=0.2\pm0.05$ nm for the dense-layer–silica interface). The model is represented in the insert for the silanated wafer and for bare silicon.

which does not damage the surface since the roughness, as measured by x-ray reflectivity, remains constant. Water spreads on this surface, thus it has a critical surface tension $\gamma_c$ larger than 73 mN/m. The value of the spreading parameter $S$ is large for this surface [an (under)estimation of $S$ is $S\sim\gamma_c-\gamma\geq 50$ mN/m]. From a chemical point of view, this surface exhibits silanol groups which allow the formation of hydrogen bonds with the oxygen atoms of the polymer chains.[44,45] The hydration of the surface is thus an important parameter.

A reflectivity curve and the corresponding electron density profile, typical for a silicon wafer, are given in Fig. 5. As the electron densities of silicon and silica are very close to one another, providing little contrast, the reflectivity curve is Gaussianlike [see formula (4)]. The measured surface roughness is $\langle z^2\rangle^{1/2}=0.42\pm0.05$ nm, which can slightly vary with each sample as can be seen on Fig. 5(b). One can determine the characteristics of the oxide layer by fitting the reflectivity curve or by ellipsometric measurements on the same sample[10,11] (the contrast between silicon and silica is good for visible light wavelengths).

### 2. *Chemical grafting of a silane monolayer*

A second controlled type of substrate is obtained by chemical grafting of a compact monolayer of octadecyltrichlorosilane (OTS) on a (111) silicon wafer, following Sagiv's procedure.[25] The critical surface tension $\gamma_c$ of this substrate is obtained from a Zisman plot[46] by measuring the contact angle for a series of liquid alcanes. $\gamma_c$ is of the order of 22–23 mN/m and thus $S$ is smaller or close to 1, but still positive.[40]

The corresponding reflectivity curve has been recorded down to $10^{-9}$, providing direct information at a scale of the order of 0.4 nm [Fig. 5(a)]. An electron density profile which yields a good fit to the data clearly contains a denser layer just under the hydrocarbon chains [Fig. 5(b)]. This layer is attributed to the Si heads of the silane molecules. The roughness of the air-chain interface and chain–dense-layer interfaces is almost identical (here $\approx 0.4$ nm), as one might expect for a single molecule, and the head-$SiO_2$ interface roughness is very low ($\approx 0.2$ nm). All that agrees with what we know about the silanation reaction:[25] a self-assembled layer builds up which is anchored on the surface by reaction with the silanol groups.

Tidswell *et al.* have recently studied these layers extensively using synchrotron radiation,[22] and have given a very precise description of their structure which is consistent with our results. Note that our data, recorded with a classical x-ray tube, allows a determination just as precise.

From the surface-diffraction data (recorded at an angle of incidence of $\theta=3$ mrad), one obtains information about the in-plane structure of the grafted layer. Here, the position of the Bragg reflection (Fig. 6) at $\psi=0.37$ rad is indicative of a spacing of $d=0.412\pm0.004$ nm. This corresponds to a densely packed hydrocarbon layer, since the area per molecule is $0.185\pm0.005$ nm$^2$, in good agreement with the electron density determined from the

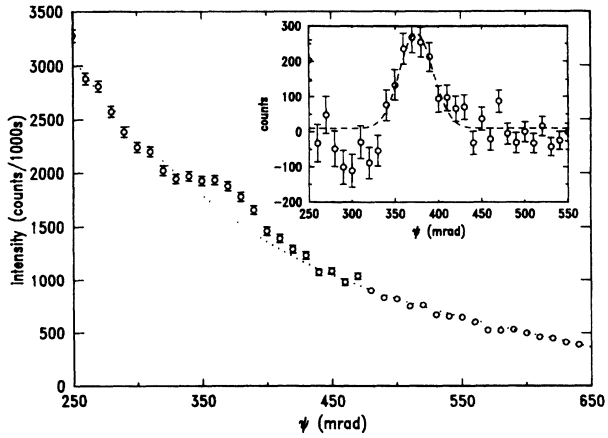


FIG. 6. Surface diffraction on a silanated wafer. In the insert the background has been substracted. The peak location is indicative of a $0.412\pm0.05$-nm spacing.

reflectivity data. Nevertheless, the correlation length is no more than a few spacings, and the layer is disordered.

### 3. *Experimental procedure*

Two different geometries have been usually considered in studies of wetting: the first is simply the spreading of a droplet on a horizontal surface and the second is the capillary rise. These are illustrated in Fig. 2.

In the first type of experiment, a droplet was deposited on a bare or silanated silicon wafer placed in a small Kapton box to prevent contamination by dust. Since the equilibrium thickness of the film is expected to be less than a nanometer, and the surface of the substrate is limited ($\sim 20$ cm$^2$), we used very tiny droplets ($V \approx 10^{-7}$ cm$^3$) in order to avoid that they reach the edge of the substrate. The volume was measured by microscopy before beginning the x-ray experiments. The droplets could be studied from right after their deposition until the final stages of wetting, sometimes reached a few months later. The chosen geometry is such that we measure the droplet thickness on a diameter (i.e., the profiles always include the center of the droplet), and the beam strikes the droplet normal to this diameter.

A second type of experiment, the capillary rise, was undertaken in order to separate the question of the growth of the molecular film from that of the vanishing of the central drop. Here, we only looked at bare silicon wafers. The polymer was contained in a small reservoir made of Teflon in which the substrate (silicon wafer) was pinned. The entire system was enclosed in a Kapton box.

Experiments were also undertaken in a sealed cell under dry $N_2$ atmosphere in order to investigate a possible role of substrate hydration. The results obtained under these conditions confirmed the generality of the previous conclusions.

## V. RESULTS

The final stages of spreading have been discussed in Ref. 13, and it was shown that, at a molecular level, the nature of the substrate played an important role. In this paper, the attention will be focused on the intermediate stages, including the determination of the droplet profiles and of the spreading kinetics. As pointed out, very small droplets ($\approx 10^{-7}$ cm$^3$) are well suited for this purpose: we could continuously investigate their spreading from right after deposition on the substrate until the final stages of spreading. PDMS of molecular weight 6500 g/mol spreading on bare silicon is our basic system and we shall present it first. The spreading of this same polymer on silanated substrates appears to be, to a large extent, quite similar. It is worth noting that these systems cover a wide range of practical situations: silica is representative of a typical oxide surface and densely packed methyl groups of organic surfaces. This allows a quite general picture of the spreading of tiny droplets.

It is generally admitted that the limit of entanglement of PDMS chains is about 13 000 g/mol.[47] A completely different dynamical behavior may occur beyond this value[48,49] and we have studied higher molecular polymers. A related open question is that of the role of the radius of gyration, which is a natural length scale in the case of polymers. We shall consider these points below.

Capillary rise experiments were undertaken to complement the information about the early stages of spreading. In the case of a system with a very low $S$ value ($\langle S/\gamma \rangle^{1/2} \sim 10^{-2}$), a scaling analysis of the upward creep of a wetting fluid shows a very rich hierarchy of phenomena with time:[50] a macroscopic meniscus is set up in a short time, a dynamic and then diffusive precursor film appears and a self-similar slow growth is reached after a few days. The time needed to reach equilibrium is prohibitive for an experimental study. This aspect has not been developed here, but we have concentrated on a surface-flow analysis. This system, including a reservoir, allows one to separate the growth of thin films from other problems.

Throughout these experiments, we did not note any contamination; i.e., the reflectivity curves remained unchanged months later on the uncovered parts of the substrates.

### A. Spreading of a droplet of molecular weight 6500 g/mol on a bare silicon wafer

#### 1. *Profile of the droplet*

The maximum thickness of the droplet is typically 30 nm by the time of the earliest x-ray experiments, and the spreading is continuously followed until the droplet is flat, a few months later. The profiles of a droplet ($V = 3.35 \times 10^{-7}$ cm$^3$) at different stages of spreading are shown in Fig. 7. These profiles can be fitted with a

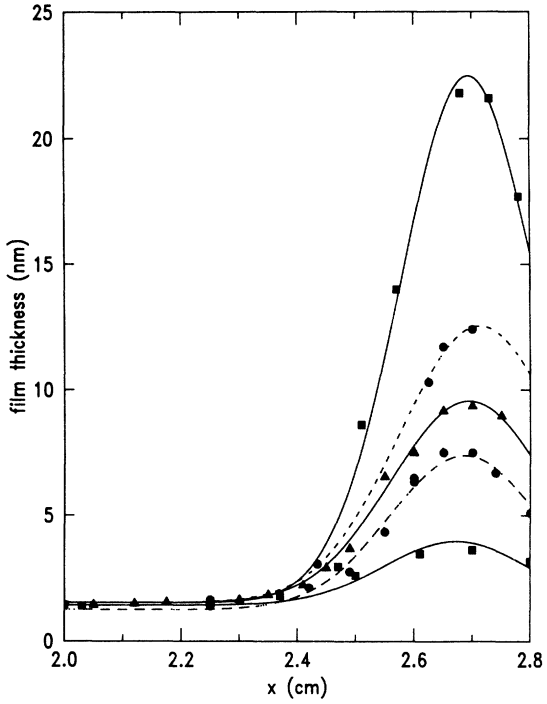


FIG. 7. Vanishing of the central part of a droplet ($V = 3.35 \times 10^{-7}$ cm$^3$) of PDMS 6500 g/mol on bare silicon and the corresponding Gaussian fits. The profile is represented at $t = 11$, 17, 21, 36, and 88 days.

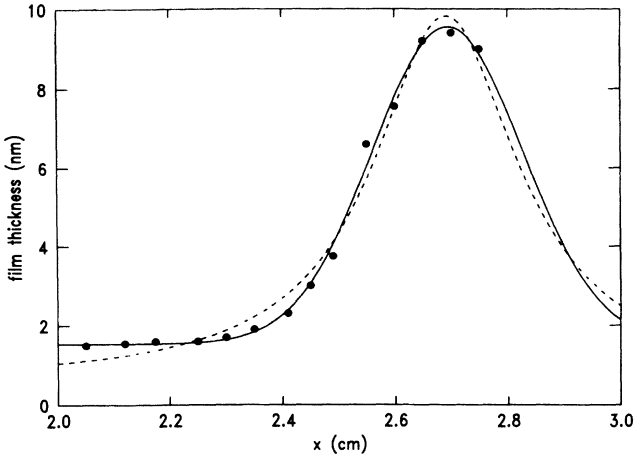


FIG. 8. Best least-squares fits to a Gaussian (solid line) and a Lorentzian (dotted line) of the droplet of PDMS 6500 g/mol ($V=3.35\times10^{-7}$ cm$^3$) on bare silicon at $t=17$ days.

Gaussian function, as well as for the other droplets which were studied ($V=2.4\times10^{-7}$ cm$^3$, $3.4\times10^{-6}$ cm$^3$, and $4.1\times10^{-7}$ cm$^3$). A Lorentzian shape has been predicted,[51] but this clearly does not agree with the experimental data (Fig. 8).

A most striking feature is that the width of the Gaussian remains relatively constant throughout the spreading (Fig. 7). More precisely, it increases much slower than $t^{1/2}$ as one would expect for a diffusion law.

In all the cases that were studied, the Gaussian part of the droplet is surrounded by a long, almost flat "tongue," shown in Fig. 9(a). (In order to avoid confusion, we shall use the word tongue when the film is molecular and precursor when it is colloidal.) Since the majority of the Gaussian part is contained within an 8 mm diameter, and the tongue extends over an area of about 10 cm$^2$, approximately nine tenths of the polymer chains (depending on the time) are contained in the tongue. Hence, the polydisperity in the chain lengths cannot give account of such an effect.

The thickness and the density of the tongue undergo a slight decrease from the foot of the Gaussian part to the edge which is rather abrupt: near the central part, the thickness is $e=1.5$ nm and the density $\rho=0.9\rho_{\text{bulk}}$ ($\rho_{\text{bulk}}$ is the electron density of bulk PDMS); over the majority of the film and near the edge, $e=1.1$ nm and $\rho\approx0.75\rho_{\text{bulk}}$. As the measured $\rho$ is the mean electron density over the illuminated area, this implies that the films are either homogeneous but not densely packed (parallel and/or normal to the surface), or dense but with holes. In all of these experiments the roughness of the substrate (bare silicon) was $0.47\pm0.05$ nm, and that of the polymer film was $0.3\pm0.03$ nm. These values were determined statistically using a series of independent measurements; for each fit these parameters were free to vary. Since these roughnesses have the same order of magnitude as the thickness, a less ambiguous way to characterize the film is to compute the surface excess quantity. The values of the density and the thickness

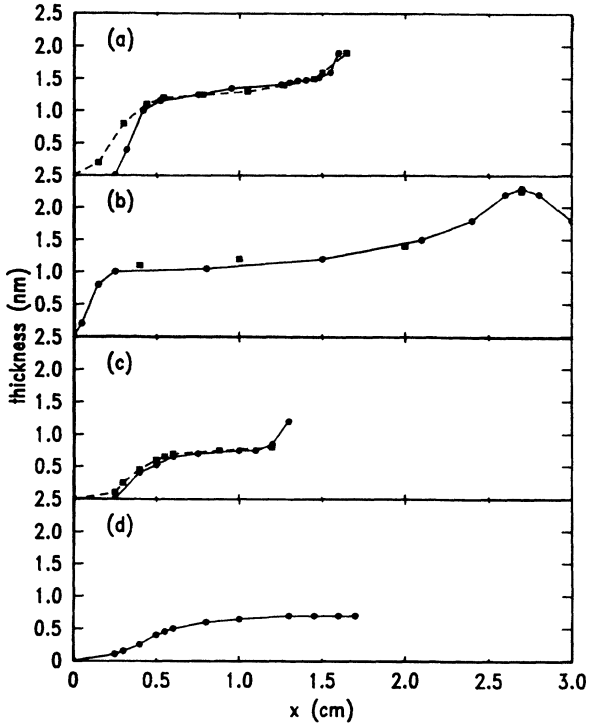


FIG. 9. (a) The "tongue" of a droplet of PDMS 6500 g/mol ($V=3.35\times10^{-7}$ cm$^3$) on bare silicon at $t=14$ and 21 days. (b) The same droplet at $t=138$ days exhibiting the "straggler" of thickness 2.2 nm. (c) The tongue of a droplet of PDMS ($V=3.4\times10^{-7}$ cm$^3$) of the same molecular weight on a silanated wafer at $t=8$ and 15 days. (d) The same droplet (the so-called "pancake") at $t=36$ days.

over the majority of the tongue are then in good agreement with a single-layer coverage of the substrate (the thickness of a polymer chain lying flat on the substrate is $\sim0.7$ nm). Note that the measured thickness ($\geq1.1$ nm) is larger than the molecular lateral dimension providing nondirect information about the conformation of the chains.

### 2. *Stages and kinetics of spreading on silicon*

*a. Very short times: birth of the "tongue."* At the beginning of the x-ray experiments, the tongue is already present, and only a slight shift of the contact line is detected at that time [Fig. 9(a)]. The first stage of the process then consists of the quick development of a molecular film with a characteristic time $\tau_1\lesssim1$ day. We observed the same characteristic features (and times) with a much larger droplet. Thus, the growth of the tongue is a general process of spreading for these systems, independent of the initial volume. This time $\tau_1$ will be again deduced by capillary rise experiments.

*b. Intermediate times: vanishing of the central bump.* The width of the droplet remaining essentially constant, the thickness of the maximum is the quantity of relevant physical significance. A plot is given in Fig. 10. During the first weeks, the variation in the height is compatible with a relaxation law and the central bump had almost

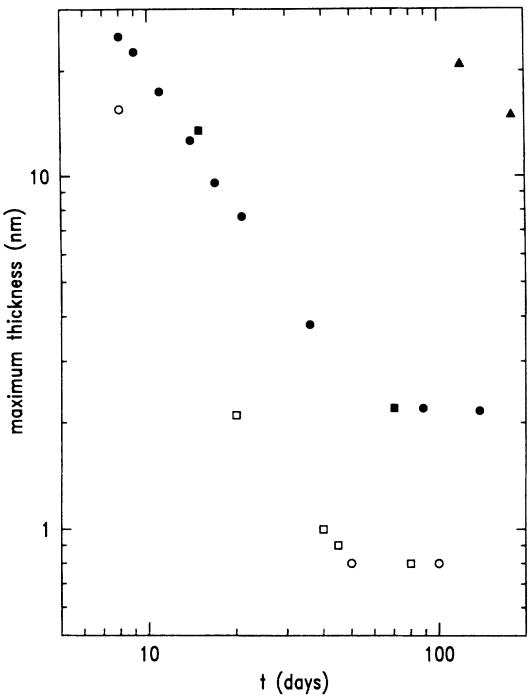


FIG. 10. Kinetics of spreading. Closed symbols: PDMS 6500 g/mol on bare silicon. ●, $V=3.35\times10^{-7}$ cm$^3$; ■, $V=4.0\times10^{-7}$ cm$^3$; ▲, $V=3.4\times10^{-6}$ cm$^3$. The points approximately fall on a straight line of slope $\approx1.1$. Open symbols: PDMS 6500 g/mol on a silanated wafer. ○, $V=3.1\times10^{-7}$ cm$^3$; □, $V=4.17\times10^{-7}$ cm$^3$.

completely vanished at a time on the order of $\tau_2\approx40$ days. This is the second characteristic experimental time of the process.

At these times, the distribution of matter in the tongue as well as the growth of the film are consistent with a diffusion law, and the entire set of data is in good agreement with a diffusion constant of $D=(7\pm5)\times10^{-7}$ cm$^2$/s. This constant is directly determined using the density and thickness profiles of the tongue to evaluate surface excess quantities. This value gives account of the diminishing of the volume remaining in the hump with the characteristic time $\tau_2$, and thus we observe mainly the vanishing of the hump into or through the tongue. Due to the difference in magnitude between $\tau_1$ and $\tau_2$, it is justified to separately study these two phenomena. The capillary rise leads to more reliable data about the early development of surface films, undistorted by geometrical factors.

Measurements of the kinetics of spreading of a much greater droplet ($V=3.4\times10^{-6}$ cm$^3$) are presented in Fig. 10.

*c. Long times: the "straggler."* Quite striking, as well, is an important slowing down of the spreading rate. The droplet for which we measured $\tau_2=40$ days did not vanish during the more than 250 days that it was followed after its deposition. A third time constant $\tau_3$ must then be introduced, characteristic of the behavior of what we shall call the "straggler," i.e., the remaining part of the hump at long times, consisting of a thicker zone ($\sim2$ nm) at the center of the droplet [Fig. 9(b)]. Schematically, the phenomena are ordered in three successive periods: quick growth of a monomolecular film, further evolution of the film due to a diffusion process, constraining the vanishing of the central bump, and the late stages. In Ref. 13 we did not observe a significantly thicker zone on the surface, as the straggler is. This may have been due to the fact that the droplet having a smaller volume ($10^{-7}$ cm$^3$) was at the really very end of spreading. Obviously, we cannot exclude that this was due to the large distance between the measurements ($\approx5$ mm).

*d. The last stage.* Towards the end of the spreading process, a monomolecular film remains on the substrate. We could measure the density of this film at different places on the substrate[13] and demonstrate that it was not homogeneous. This flat film is not an equilibrium state and the spreading does not stop. The tongue becomes more and more diffuse, and the cohesion of the liquid is broken, i.e., cohesive forces are screened by the interactions with the substrate. In our previous study, we established that, in this case, the theoretical picture of the pancake[5,6] is not relevant.

### B. Spreading of a droplet of molecular weight 6500 g/mol on a silanated silicon wafer

This system behaves much like the previous one; two significant differences, however, must be underlined. In the case of spreading on silica, we were able to distinguish three different steps with their characteristic times. Only the first two (growth of the monomolecular film and vanishing of the central bump) are observed with the silanated substrate, i.e., there is no straggler. The nature of the final state has been shown to be very different.[13] As previously, the monomolecular tongue grows very quickly and is already present when beginning the x-ray experiments [Fig. 9(c)]. The central part of the droplet [Fig. 11(a)] can be fitted with a Gaussian function, just as in the case of bare silicon substrates, and the characteristic time $\tau_2$ associated to its vanishing has the same order of magnitude (20 days for $V\approx3\times10^{-7}$ cm$^3$). In summation, the early stages of spreading appear to be quite similar.

The structure of the tongue, however, is slightly different: this is a flat film, only 0.7 nm thick, with an abrupt edge [represented in Fig. 9(c) at $t=8$ days and $t=15$ days]. The thickness is that of the polydimethylsiloxane chain with the methyl groups randomly oriented. Its density cannot be accurately determined since it is very close to that of the densely packed hydrocarbon chains covering the substrate. This lack of contrast, which nevertheless indicates that the film is dense, prevents us from determining accurately a diffusion constant.

The most significant difference from the previous case is related to the later development. The droplet represented on Fig. 11(a) ($V=3.1\times10^{-7}$ cm$^3$) had completely spread within one month after its deposition, leaving a monomolecular flat film ($e=0.7$ nm) with well defined edges on the substrate. This film was discussed in

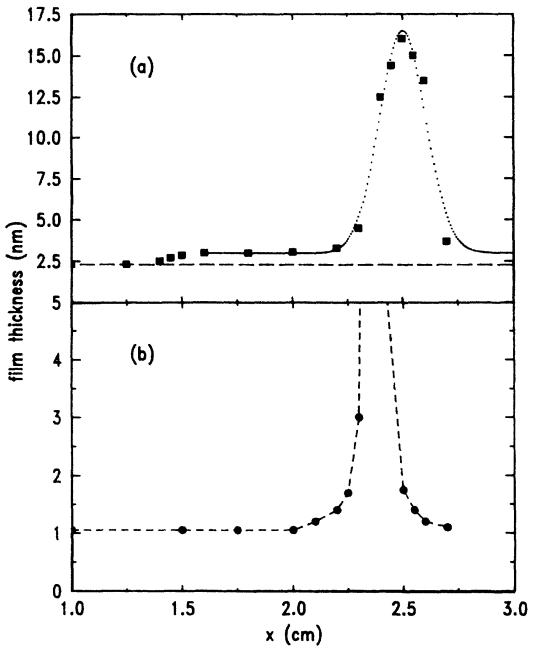


FIG. 11. (a) Droplet of PDMS 6500 g/mol on a silanated wafer ($V=3.1\times10^{-7}$ cm$^3$). The thickness of the silane layer is indicated by a dotted line. (b) Droplet of PDMS 79 000 g/mol ($V=4.2\times10^{-7}$ cm$^3$) on bare silicon. In the central part of the droplet, the very steep slope does not allow us to extract information from the data.

our previous study. It has been established[13] that the picture of the pancake is relevant: an equilibrium state was reached, consisting of a dense liquid film (but the thickness of this film was not in the colloidal range). This is confirmed by the results of Fig. 9(d) which shows the equilibrium state, whose thickness corresponds to the monomer width of the PDMS chain. The spreading stops, and the equilibrium system is a finite, flat liquid film, with well defined edges. This state is in equilibrium, and the cohesion of the liquid is not broken.

Obviously, these results concerning the spreading of a single polymer on two different substrates strongly support the fact that the differences between the two situations are due to the nature of the polymer-solid interaction. Moreover, it enables us to rule out any argument based on nonintrinsic peculiarities (e.g., polydispersity) to give an account of the different experimental observations.

### C. Spreading of higher molecular weight polymer droplets on bare silicon

These experiments were undertaken at first in order to investigate dynamical effects as well as a possible role of the radius of gyration, which is a natural characteristic length for polymers. These higher-molecular-weight polymers (33 000 g/mol and 79 000 g/mol) are entangled, and, due to the higher viscosity, the kinetics are much slower than in the previous cases (see Table I for the sample characteristics). The thicknesses and gradients remain large, and no complete profile of a droplet could be determined since the contrast vanishes at the center, due to the too-high slope [Fig. 11(b)]. In this case, we were only able to measure the characteristics of the tongue: the mean density is such that $0.55\rho_{\text{bulk}} \lesssim \rho \lesssim 0.65\rho_{\text{bulk}}$. The thickness $e \simeq 1.1$ nm, and the roughness $\langle z^2_{\text{PDMS/air}} \rangle^{1/2} \approx 0.3$ nm are the same as for the case of molecular weight 6500 g/mol. These values are indicative of a less complete coverage of the surface than previously. Moreover, no abrupt edge could be detected, the amount of polymer decreasing slowly at the tip. The polydispersity (Table I) is lower than in the case of the shorter chains samples we have used, therefore, this wide edge can probably be considered as a molecular-weight effect.

Whereas the radius of gyration $R_g$ is much greater than in the case of PDMS of molecular weight 6500 g/mol, the thickness of the tongue is, as in that previous case, larger but of the order of magnitude of the molecular width. Clearly, $R_g$ is not a relevant parameter of the system. These results are in contrast with the theoretical model of Ref. 49.

### D. Results on the capillary rise

#### 1. *Growth of the monomolecular film*

The aim of these experiments was to get complementary information about the growth of the tongue at short times. Two polymer samples of molecular weights 9600 g/mol and 50 000 g/mol were used, the last one being entangled. Their characteristics are detailed in Table I. The substrate was a bare silicon wafer and the beam struck the surface 3 cm above the liquid surface for this

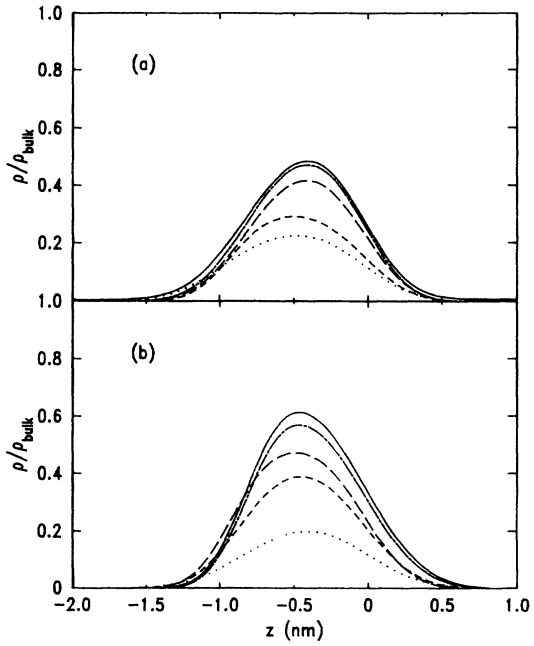


FIG. 12. Capillary rise experiment. Polymer distribution normal to the surface of the substrate. $z=0$ is the location of the silicon surface: $z \gtrsim 1$, bulk silicon; $z \lesssim -1.5$, air. (a) Molecular weight 50 000 g/mol and (b) molecular weight 9000 g/mol.

first kind of experiment. Reflectivity curves were continuously recorded in order to investigate the growth of the film. Representative polymer distributions along the normal to the surface are given in Fig. 12. The amount of polymer on the surface was determined at each time using formula (5), and this quantity was used to analyze the results.

The experimental data agree with a diffusion law; the diffusion constants were determined to be $D=1.5\times10^{-4}\pm5\times10^{-5}$ cm$^2$s$^{-1}$ in the first case and $D=10^{-4}\pm5\times10^{-5}$ cm$^2$s$^{-1}$ in the second case. These constants are consistent with our previous estimation since a time $\tau_1\approx1$ day was required to cover $\approx10$ cm$^2$ of substrate. Rather surprisingly, the entangled chains of molecular weight 50 000 g/mol and these of molecular weight 9000 g/mol creep at approximately the same velocity, within the experimental incertitude. This feature suggests that the phenomena governing the growth of the tongue is the diffusion of disentangled molecules lying flat on the surface governed by monomer mobility, rather than the disentanglement itself.

### 2. *Profile of the precursor film*

The characterization of the precursor film was not the main purpose of this experiment, but it provides interesting information about a system whose behavior is scaled by macroscopic phenomena. The experimental system is the same as previously, but the sample is translated in order to investigate different heights above the reservoir.

The region above the meniscus is represented in Fig. 13 a few days after the beginning of the experiment. The data are well fitted with an $x^{-1}$ profile, and the agreement is much better than with a $x^{-2}$ profile. Such an hyperbolic film is expected[50] near the bulk surface of the liquid, the crossover length with the diffusive film being related to the meniscus velocity.

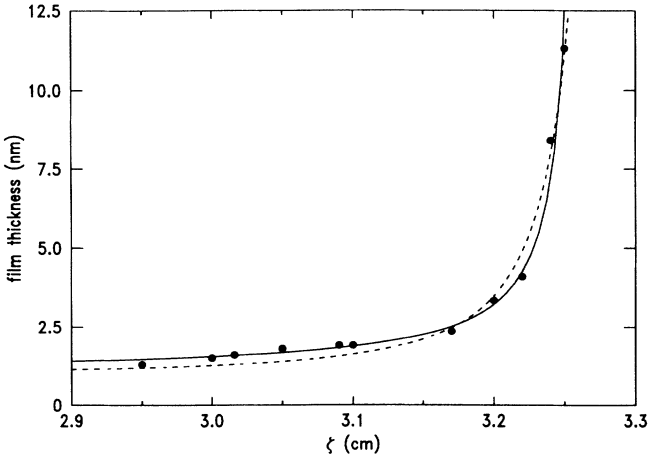


FIG. 13. Capillary rise experiment. Precursor film with PDMS 6500 g/mol on bare silicon. Solid line, best $x^{-1}$ fit; dotted line, best $x^{-2}$ fit.

## VI. DISCUSSION

If few experimental results concerning spreading at a molecular scale are available, the theoretical treatment is even more scarce. We shall discuss the experimental data using a rough model of surface flow which is only expected to exhibit the most important trends without completeness. The main problems to be discussed are the fast growth of the tongue and its molecular structure, the profile of the central bump, and, finally, the late stages, which are related to the problem of surface-polymer interactions. The question of surface roughness will be discussed.

### A. Transport processes in the tongue

#### 1. *Surface flow*

The fast development of a large and flat film ahead of the droplet or ahead of the meniscus is one of the most striking features of the spreading of PDMS, as observed by x-ray reflectivity.

The two cases of films of colloidal or molecular thickness are different. Following Ref. 50, when the experiment involves a reservoir (e.g., the capillary rise), the rate of spreading is scaled by macroscopic phenomena, and an hyperbolic "adiabatic" precursor film can be observed. This film becomes diffusive and a crossover length can be calculated which depends on the velocity of the meniscus. Such an hyperbolic film was observed (Fig. 13).

With tiny droplets, no macroscopic reservoir is available, and we have shown that the film is diffusive. It was established in Ref. 41 that PDMS behaves as a liquid with a bulk viscosity down to 3 nm, but, obviously in the case of monomolecular films, the flow process on the solid is more appropriately considered as a surface diffusion process than as hydrodynamic.[52] The purpose of the crude model, presented below, is to give account of the fast growth of the diffusive tongue, taking into account the surface energy gained during spreading.

Let us compare the forces acting on the system. The equilibrium state of a droplet in the theory of de Gennes and Joanny is a film called pancake, whose thickness $e_p$ results from a balance between two antagonist effects: the disjoining pressure tends to thicken the film whereas the spreading forces tend to make it thinner. One obtains $P(e)+e\Pi(e)=S$, where $P$ is the energy per unit surface associated to long-range forces, and $\Pi=-dP/d\zeta$ is the disjoining pressure. For van der Waals interactions, this statement leads to the pancake formula $e_p=\langle A/(4\pi S)\rangle^{1/2}$. In the case of silanated wafers, using $A=10^{-20}$ J and $S=1$ mN/m, one can estimate the equilibrium thickness $e_p$ which is of the order of magnitude of the molecular width of the monomer ($e_m=0.7$ nm), whereas $e_p\ll e_m$ for bare silicon. Thus, capillary forces are expected to always overcome the dispersive forces and one can make an estimation of the velocity of the edge, balancing dissipation against the excess energy $S$.[53] [In Ref. 5, an equivalent treatment was developed, assuming a Poiseuille flow. A relation was found between the velocity of the edge and the disjoining pressure gradient,

and $S$ was introduced as a limiting condition, since a precursor film must be truncated at a thickness $e_p(S)$.]

#### 2. Role of the spreading parameter

The molecular flow on the surface can be roughly described using a simple model: The transport of molecules is considered as a rate process,[54–58] and an energy barrier opposes to the hopping, leading to a Eyring formula for the rate constant $k$ which is the number of times the hopping occurs per second (the effective viscosity for the surface flow process is $\eta_{\text{eff}} \propto k^{-1}$). If $\delta$ is the magnitude of the jump for the elementary unit of flow, $k\delta$ is the (randomly oriented) velocity of such units. Since an energy $S$ is gained per unit area when covering the surface by a thin film of molecules, the barrier is distorted and nonsymmetric (the process is activated), whereas in a pure diffusion process, the barrier is symmetric but the density of molecules is different on each side. Assuming that the process is circularly symmetrical, the energy gained when jumping from a position of the contact line to another is $2\pi R\,\delta S$, implicating $2\pi R\rho_s$ elementary flow units ($\rho_s$ is the surface density of such units). Hence, the height of the barrier is diminished by $\Delta U \propto S$ for when the molecules jump forward and increased by the same amount for hopping in the opposite direction.[55,56] This leads to a rescaling of the probability of hopping in the forward direction and thus the velocity of the edge is proportional to $S/\eta_{\text{eff}}$. This rough model has to be carefully examined, but displays satisfactory trends: The velocity of the edge is found to be proportional to the spreading parameter $S$ and inversely proportional to the effective viscosity. Also as pointed out in Ref. 49, the mobility of the monomer on the substrate ($\propto \eta_{\text{eff}}^{-1}$) is an important parameter. It is rather difficult to compare the processes which occur on bare and on silanated silicon wafers: $S$ is larger for bare silicon but the friction is also expected to be greater, the chains being more strongly bonded to the substrate by hydrogen bonds. Since the two effects are antagonistic, no general conclusion can be drawn, but, experimentally, the second appears to be slightly more important. The effect of the spreading parameter $S$ on the spreading rate can be estimated as below.

#### 3. Relation with surface diffusion

When the droplet is almost flat, the molecular flow has to relax towards a true diffusion process. As a matter of fact, this diffusion process can only occur if the cohesive forces in the film are screened. This is the case on bare silicon wafers but not for silanated ones (on which the spreading stops). The diffusion constant has been determined in the bare silicon case, and we find $D=(7\pm5)\times10^{-7}\ \text{cm}^2/\text{s}$.

Using the simple model of surface flow, one can determine the ratio of the diffusion constant for the surface-energy-driven process to that for the true diffusion process which is $2S/(k_B T\rho_S)$. As previously, $\rho_S$ is the surface density of flow units and this expression (analogous to an Einstein relation) is expected to have a more general validity, based on energetic considerations, than the underlying model. A rough estimation of this quantity provides a ratio of 100 or more for a dense film with $S\sim50$ mN/m (bare silicon). Thus, the activation of the surface diffusion process from the energy gained by spreading is consistent with the fast growth of the tongue. Let us remark that if the transition from a flow dominated by surface energy to a true surface diffusion accounts for the slowing down of the process with the two characteristic times $\tau_1$ and $\tau_2$, it cannot completely explain the persistence of a thicker zone at the center of the drop (which should disappear within $\sim20$ days). A more detailed discussion of the liquid-substrate interactions is required for this purpose.

### B. The profile of the central bump

At thicknesses greater than 3 nm,[41] PDMS 6500 g/mol can be considered as having its bulk hydrodynamic properties. Neglecting all forces but those included in the disjoining pressure, the equation to be solved in the lubrication approximation is then

$$\frac{\partial\zeta}{\partial t}=-\frac{1}{r}\frac{\partial}{\partial r}\left[r\frac{\zeta^3}{3\eta}\frac{\partial\pi}{\partial\zeta}\frac{\partial\zeta}{\partial r}\right], \tag{6}$$

where $\zeta$ is the local thickness of the droplet and $\eta$ the liquid viscosity. The meaning of Eq. (6) is that the rate of flow is due to a disjoining pressure gradient. Suitable conditions must be introduced specifying the flow of liquid in the tongue and the balance of energy (taking into account the spreading parameter $S$). As a matter of fact, a quantitative treatment is very uneasy, since, firstly, the exact structure of disjoining pressure is largely unknown, and, secondly, an hydrodynamic treatment must be related to the effects of surface diffusion in the tongue. Two solutions of the nonlinear equation (6) are worth mentioning even if they are necessarily approximated for the present case.

This equation has been discussed[51] in the case of microscopic droplets of van der Waals liquids. A self similar solution was found consisting of a Lorentzian profile having an exponential decrease of the thickness at early times and an exponential increase of the radius. Since this equation is not valid at molecular thicknesses, the comparison between Gaussian and Lorentzian shapes is without meaning (this is all the more true, since these shapes are distinguished at small thicknesses for which the structural part is the most important), but clearly an exponential increase of the width is inconsistent with the data.

Equation (6) has also been used to study the relaxation toward equilibrium. The equation can be linearized yielding a diffusion equation whose solution is decomposition[6] in modes. At long times, the slowest mode is assumed to be the most important one. The solution is then a Bessel function with an exponentially decreasing thickness. For a given mode, the width of the bump remains constant, but the predicted shape cannot fit the data.

The experimental results, which are strongly inconsistent with an exponential or $t^{1/2}$ (diffusion-law) increase of the droplet width, suggest a mechanism such as the

following: the liquid is drawn into the tongue while molecular forces oppose the thinning down of the central bump. Note that the measured diffusion coefficient in the tongue is $7\times10^{-7}$ cm$^2$/s, whereas Eq. (6) yields a diffusion coefficient of $\approx10^{-8}$ cm$^2$/s for $A=10^{-20}$ J, $\eta=0.05$ Pa s, and $\zeta=10$ nm. In that sense, the case of microscopic droplets is completely different from that of Ref. 26, for which the precursor film was scaled by the macroscopic velocity of the edge. Here, on the contrary, the droplet is broken up by diffusion of the tongue. It is thus tempting to develop a simple argument such as the following. A determined amount of polymer diffuses from the hump into the tongue during each time unit. Using the separation between the characteristic times of the two processes [diffusion in the tongue and hydrodynamic flow as described by Eq. (6)], one can replace $\partial\zeta/\partial t$ in Eq. (6) by the quantity of polymer $\Phi$ lost by the central bump due to diffusion into the tongue, and this amounts to take into account the limit condition. As we know from the discussion of Eq. (6), this determines a disjoining pressure gradient, i.e., the droplet profile. The modified Eq. (6) can be solved in the case of a van der Waals liquid ($\Pi=A/6\pi\zeta^3$) and one obtains

$$\zeta=\zeta_0\exp\left[-\frac{3\pi\eta\Phi}{2A}r^2\right],$$

which is a Gaussian profile whose width, proportional to $\langle A/\eta\Phi\rangle^{1/2}$, is due to a balance between disjoining pressure and diffusion in the tongue. Note that this expression is analogous to that of the line shape of the precursor film:[5] $\zeta=\langle A/6\pi\eta U\rangle^{1/2}x^{-1}$, the velocity of the macroscopic front $U$ being replaced by $\Phi$ related to the surface diffusion process. Now, it is possible to evaluate $\Phi$ by determining the total amount of matter lost by the droplet. During each time unit, the tongue covers an area $4\pi D$ which contains a volume $4\pi De_t$ lost by the droplet, where $e_t$ is the tongue thickness. This is in good agreement with the data of Fig. 10, since the diminishing of the maximum thickness, and thus that of the droplet volume, were found to be approximately proportional to the time. With $D=7\times10^{-7}$ cm$^2$/s and $e_t=10^{-9}$ m, one finds $\Phi\approx3\times10^{-14}$ m/s for an area $3\times10^{-5}$ m$^2$. Using then $A=10^{-20}$ J and $\eta=0.05$ Pa s, the half-width at half maximum is found to be 1 mm.

This result indicates that the width of the droplet could be due to the diffusion in the tongue constrained by long-range forces. This estimation is, of course, rather rough, since the flow has not been considered as truly three dimensional, and $\Phi$ has not been calculated on a microscopic basis.

### C. The role of substrate-polymer interactions

This section is devoted to the discussion of the aspects of the spreading more particularly related to the substrate. From a general point of view, the substrate-liquid interactions are described using a disjoining pressure[58] which, in the present case, is expected to have a long-range molecular component due to dispersive forces and a structural component including the effects of hydrogen bonding. In the case of silanated wafers, the substrate is covered by a 2-nm thick, dense hydrocarbon layer, and the interactions are mainly due to van der Waals forces. Conversely, short-range forces will play a major role for very thin films of PDMS on bare silicon surfaces. The effect of such forces on wetting phenomena is well known since the work of Zisman and is illustrated by the case of autophobic liquids[59] which are unable to spread over their own adsorbed films. Shafrin and Zisman[60] have studied polydimethylsiloxane from this point of view. They concluded that the methyl groups exposed by the silicon film are sufficiently closed packed to shield the Si—O linkages effectively from the wetting interface, leading to a lower critical surface tension.

These conclusions are in good agreement with our measurements: the thickness of the microscopic film implies that the chains should lie flat on the substrate, whatever the molecular weight, and, since the coverage is dense, thus exhibit an efficient methyl layer. Actually, the thickness measured on bare silicon (1.5 nm) is larger than that on silanated surfaces (0.7 nm). Since the film is monomolecular in both cases, this suggests that the chains are constrained on bonding sites on silicon, hindering the chains from lying completely flat. The lower density measured with longer polymer chains may also be related to the silica-PDMS interactions: Two-dimensional ideal chains would not have this behavior since their mean-squared radius is proportional to the monomer number.

Another point which may be related to the substrate polymer interactions, and more particularly to an orientation of the methyl groups, is the retention, at the end of the spreading process of a thicker part (2.2 nm) on bare silicon wafers. A general discussion cannot be carried out due to a lack of information about the disjoining pressure, but from this point of view, it should be interesting to consider an equilibrium between two very thin films: the tongue and the straggler.

Qualitatively, the phenomena can be understood as follows: the first layer of siloxane chains (1.5 nm), hydrogen bonded to the substrate, exhibits methyl groups which considerably diminish the critical surface tension so that this low-$S$ surface is not very different from that of a silanated substrate. As we know, an equilibrium state for spreading is reached on this surface, which is a film of molecular thickness (0.7 nm) in which cohesion prevails over diffusion (Sec. V B). Since the two situations are quite close to one another (a monomolecular film on silane and on a first PDMS monolayer), this equilibrium state is indicative of what can be expected on bare silicon and could explain the very long times required to completely spread the droplet.

An important characteristic of the substrates is that they exhibit a low but non-negligible roughness. Since the thickness of the monomolecular films is of the order of magnitude of the mean roughness of the different substrates, the interfacial roughnesses must be intimately taken into account. A general study of the role of roughnesses on the dynamics of wetting at a microscopic level has not yet been either theoretically nor experimentally undertaken. Of course, x-ray reflectivity is the most adapted technique for this last task.[61] Concerning statics,

the correlation between the roughnesses at the two interfaces depends on whether the film thickness is greater than a certain healing length or not.[62] In the first case, the interfaces are not correlated, and, in the second, they are correlated. All of the experimental film roughnesses ($0.3\pm0.03$ nm) were smaller than the substrate ones ($>0.4$ nm). This suggests that the spectrum of surface roughness involves spatial frequencies on the order of the inverse nanometer: the roughness wavelength must be small, so that the roughness can be healed by the thin polymer layer. For a van der Waals liquid, a surface roughness is healed if its wavelength $\Lambda$ is such that $\Lambda < \zeta^2(2\pi\gamma/A)$, where $\zeta$ is the film thickness.[63] In the present case, this would lead to $\Lambda \approx 5$ nm (with $A = 10^{-20}$ J), a value which is, of course, only indicative.

## VII. CONCLUDING REMARKS

The role of very thin films in wetting has been evidenced, and the leading mechanism to spreading is shown to be surface diffusion for a large number of systems. Beyond the similar trends displayed by the cases of low- and high-energy surfaces, the sensitivity of x-ray reflectivity allows the detection of differences which are indicative of a different behavior at the molecular level due to the different liquid-solid interactions. This allows a classification into two basically different categories: in the first case, the cohesion of the liquid has to be taken into account, whereas in the second, it is screened. X-ray reflectivity was shown to be an original and powerful tool in this field of physical chemistry allowing a complete determination of the behavior of very thin wetting films. It appears very interesting to consider other open questions. The case of volatile liquids, for example, has been given little attention;[1] very challenging as well is the case of very low spreading parameters for which "thin" films should be thicker than molecular.

## ACKNOWLEDGMENTS

We have greatly benefited from the ideas and suggestions of P. G. de Gennes and F. Brochard and we wish to thank them most gratefully. We appreciate fruitful discussions with P. Silberzan who also provided many of the samples. C. Strazielle and P. Auroy fractionated the polymer samples. We are grateful to C. Blot and D. Luzet for their kind assistance, and to A. Braslau and F. Rieutord for a very critical reading of the manuscript.

[1] A. Marmur, Rev. Phys. Appl. **23**, 1039 (1988).
[2] A. Marmur, Adv. Colloid Interface Sci. **19**, 75 (1983).
[3] W. B. Hardy, Philos. Mag. **38**, 49 (1919).
[4] D. Ausséré, A. M. Picard, and L. Léger, Phys. Rev. Lett. **57**, 2671 (1986).
[5] P. G. de Gennes, Rev. Mod. Phys. **57**, 827 (1985).
[6] J. F. Joanny, thése d'etat, Université Paris VI, 1985.
[7] H. Ghiradella, W. Radigan, and H. L. Frish, J. Colloid Interface Sci. **51**, 522 (1975).
[8] A. Marmur and M. D. Lelah, J. Colloid Interface Sci. **78**, 263 (1980).
[9] W. D. Bascom, R. L. Cottington, and C. R. Singleterry, in *Contact Angle, Wettability and Adhesion,* Vol. 43 of *Advances in Chemistry Series,* edited by F. M. Fowkes (American Chemical Society, Washington, D.C., 1964), p. 355.
[10] L. Léger, M. Erman, A. M. Guinet-Picard, D. Ausséré, and C. Strazielle, Phys. Rev. Lett. **60**, 2390 (1988).
[11] L. Léger, M. Erman, A. M. Guinet-Picard, D. Ausséré, C. Strazielle, J. J. Benattar, F. Rieutord, J. Daillant, and L. Bosio, Rev. Phys. Appl. **23**, 1047 (1988).
[12] D. Beaglehole, J. Phys. Chem. **93**, 893 (1989).
[13] J. Daillant, J. J. Benattar, L. Bosio, and L. Léger, Europhys. Lett. **6**, 431 (1988).
[14] L. Névot and P. Croce, Rev. Phys. Appl. **15**, 761 (1980).
[15] A. Braslau, M. Deutsch, P. S. Pershan, A. H. Weiss, J. Als-Nielsen, and J. Bohr, Phys. Rev. Lett. **54**, 114 (1985).
[16] A. Braslau, P. S. Pershan, G. Swislow, B. M. Ocko, and J. Als-Nielsen, Phys. Rev. A **38**, 2457 (1988).
[17] R. M. Richardson and S. J. Roser, Liq. Cryst. **2**, 797 (1987).
[18] J. Daillant, L. Bosio, J. J. Benattar, and J. Meunier, Europhys. Lett. **8**, 453 (1989).
[19] D. C. Bisset and J. Iball, Proc. Soc. London Sect. A **67**, 315 (1954).
[20] F. Rieutord, J. J. Benattar, L. Bosio, P. Robin, C. Blot, and R. de Kouchkovsky, J. Phys. (Paris) **48**, 679 (1987).
[21] M. Pomerantz, A. Segmüller, L. Netzer, and J. Sagiv, Thin Solid Films **132**, 153 (1985).
[22] I. M. Tidswell, B. M. Ocko, P. S. Pershan, S. R. Wasserman, and G. M. Whitesides (unpublished).
[23] A. Bruson, M. Piecuch, and G. Marchal, J. Appl. Phys. **58**, 1229 (1985).
[24] F. Rieutord, J. J. Benattar, R. Rivoira, Y. Lepêtre, C. Blot, and D. Luzet, Acta Crystallogr. Sect. A (to be published).
[25] J. Gun and J. Sagiv, J. Colloid Interface Sci. **112**, 457 (1986).
[26] P. G. de Gennes, C. R. Acad. Sci. Ser. II **298**, 111 (1984).
[27] H. Hervet and P. G. de Gennes, C. R. Acad. Sci. Ser. II **299**, 499 (1984).
[28] R. W. James, *The Optical Principles of the Diffraction of X-rays* (Bell, London, 1948), p. 135.
[29] J. D. Jackson, *Classical Electrodynamics,* 2nd ed. (Wiley, New York, 1975), p. 418.
[30] E. S. Wu and W. W. Webb, Phys. Rev. A **8**, 2065 (1973).
[31] M. Born and E. Wolf, *Principles of Optics,* 6th ed. (Pergamon, London, 1980), p. 40.
[32] D. W. Oxtoby, F. Novak, and S. A. Rice, J. Chem. Phys. **76**, 5278 (1982).
[33] E. A. Guggenheim, *Thermodynamics: An Advanced Treatment for Chemists and Physicists* (North-Holland, Amsterdam, 1967).
[34] M. Born and E. Wolf, *Principles of Optics,* 6th ed. (Pergamon, London, 1980), p. 491.
[35] W. C. Marra, P. Eisenberger, and A. Y. Cho, J. Appl. Phys. **50**, 6927 (1979).
[36] K. Kjær, J. Als-Nielsen, C. A. Helm, L. A. Laxhuber, and H. Möhwald, Phys. Rev. Lett. **58**, 2224 (1987).
[37] P. Dutta, J. B. Peng, B. Lin, J. B. Ketterson, M. Prakash, P. Georgeopoulos, and S. Ehrlich, Phys. Rev. Lett. **58**, 2228 (1987).
[38] G. H. Vineyard, Phys. Rev. B **26**, 4146 (1982).
[39] M. Brunel and F. de Bergevin, Acta Crystallogr. Sect. A **42**, 299 (1986).
[40] These measurements have been performed by P. Silberzan.

[41]R. G. Horn and J. N. Israelashvili, Macromolecules **21**, 2836 (1988).
[42]J. R. Vig, J. Vac. Technol. A **3**, 1027 (1985).
[43]J. R. Vig, in *Treatise on Clean Surface Technology,* edited by K. L. Mittal (Plenum, New York, 1987), Vol. I, p. 1
[44]B. V. Derjaguin, V. V. Karasev, I. A. Lavygin, I. I. Skorokhodov, and E. P. Khromova, in *Research in Surface Forces* (Consultants Bureau, New York, 1975), Vol. 4, p. 520.
[45]J. P. Cohen-Addad, C. Roby, and M. Sauviat, Polymer **26**, 1231 (1985).
[46]W. A. Zisman, in *Contact Angle, Wettability and Adhesion,* Vol. 43 of *Advances in Chemistry Series,* edited by F. W. Fowkes (American Chemical Society, Washington, D.C., 1964), p. 1.
[47]R. R. Rahalker, J. Lamb, G. Harrison, A. J. Barlow, W. Hawtorn, J. A. Semlyen, A. M. North, and R. A. Pethrick, Proc. R. Soc. London Ser. A **394**, 207 (1984).
[48]F. Brochard and P. G. de Gennes, J. Phys. (Paris) **45**, L-597 (1984).
[49]R. Bruinsma (unpublished).
[50]J. F. Joanny and P. G. de Gennes, J. Phys. (Paris) **47**, 121 (1986).
[51]P. G. de Gennes, C. R. Acad. Sci. Ser. II **298**, 475 (1984).
[52]G. F. Teletzke, H. T. Davies, and L. E. Scriven, Chem. Eng. Commun. **55**, 41 (1987).
[53]F. Brochard, C. Redon, and F. Rondelez, C. R. Acad. Sci. Ser. II **306**, 1143 (1988).
[54]S. Glasstone, K. J. Laidler, and H. Eyring, *The Theory of Rate Processes* (McGraw Hill, New York, 1981), p. 477.
[55]B. W. Cherry and C. M. Holmes, J. Colloid Interface Sci. **29**, 175 (1969).
[56]T. D. Blake and J. M. Haynes, J. Colloid Interface Sci. **30**, 423 (1969).
[57]E. Ruckenstein and C. S. Dunn, J. Colloid Interface Sci. **59**, 135 (1977).
[58]H. C. Kang and H. Weinberg, J. Chem. Phys. **90**, 2824 (1989).
[59]B. V. Derjaguin, N. V. Churaev, and V. M. Muller, *Surfaces Forces* (Consultants Bureau, New York, 1987), p. 25.
[60]W. A. Zisman, in *Contact Angle, Wettability and Adhesion,* Vol. 43 of *Advances in Chemistry Series,* edited by F. M. Fowkes (American Chemical Society, Washington, D.C., 1964), p. 23.
[61]E. G. Shafrin and W. A. Zisman, in *Contact Angle, Wettability and Adhesion,* Vol. 43 of *Advances in Chemistry Series,* edited by F. M. Fowkes (American Chemical Society, Washington, D.C., 1964), p. 149.
[62]S. K. Sinha, E. B. Sirota, and S. Garoff, Phys. Rev. B **38**, 2297 (1988).
[63]D. Andelman, J. F. Joanny, and M. O. Robbins, Europhys. Lett. **7**, 731 (1988).